

High temperature superconducting tape with a current flow diverter architecture for fault current limitation in a high voltage direct current grid

Christian Lacroix and Frédéric Sirois, *Senior Member, IEEE*

Abstract—This paper presents a 1D electrothermal model that simulates the quench behavior of a superconducting fault current limiter (SFCL) in a high voltage direct current (HVDC) electric power transmission system. The model solves the heat equation through the thickness of a high temperature superconducting (HTS) tape at the location of a hot spot. Using the normal zone propagation velocity (NZPV) obtained from a distinct 3D electrothermal model, the quench dynamics in SFCLs can be predicted, which allows calculating the fault current level over time. The model was used to compare the performance of three promising tape architectures for use in HVDC electric networks. Calculations indicate that the insertion of a current flow diverter (CFD) in the tape architecture allows decreasing the fault current level and reducing the temperature elevation thanks to the increased NZPV.

Index Terms—Fault current limiters, High temperature superconductors, High voltage direct current transmission systems, Finite element analysis, Hot spots.

I. INTRODUCTION

Superconductor fault current limiters (SFCLs) are considered as one of the most promising applications of high temperature superconducting (HTS) tapes. While actual commercial HTS tapes are suitable for designing SFCL for medium-voltage network (50 kV/m fault lasting 50 ms), it is necessary to increase the electric field of REBCO tapes under limitation (up to 150 V/m) in order to implement a SFCL that can be used in a HVDC grid (voltage above 300 kV) that is not excessive in terms of size and cost. The H2020 European project FASTGRID aims at developing the best conductor design that fulfill these requirements [1].

In order to ensure the reliability of a SFCL device, the HTS tape must first withstand a clear fault. In the present case, this corresponds to apply an electric field of 150 V/m for 50 ms. In order to limit the increase in temperature of the tape during a clear fault, the tape must possess a sufficient thermal mass, which is generally obtained by adding a thick shunt [2].

Another scenario to be considered is the development of a hot spot [3]. At present time, commercial HTS tapes possess local critical current I_c that vary along their length (approximately +/-20% of variation). This variation is inherent to the

fabrication process. In the case of a prospective fault current that corresponds to the minimum local I_c of the tape, only a small zone will quench (called hot spot). Considering the low normal zone propagation velocity (NZPV) of commercial HTS tapes, a local destruction of the tape at the hot spot location thus becomes very likely. Besides increasing the homogeneity of I_c by improving the fabrication process, another solution to mitigate the hot spot issue is to add a conductive shunt in order to reduce the Joule losses [2].

Another solution is to homogenize the quench by increasing the NZPV of HTS tapes [4]. A promising way to increase the NZPV is the so-called current flow diverter (CFD) concept [5], [6], [7]. In the CFD concept, a highly resistive layer that partially covers the HTS-Ag interface is added, which forces the current to pass by the edges of the HTS tape.

Alternatively, the use of a sapphire substrate instead of a Hastelloy substrate is attractive because it possesses a much higher thermal conductivity at cryogenic temperatures. Therefore, it dissipates more efficiently the local heat generated in a quenched zone. Furthermore, a higher NZPV was observed on YBCO films grown on a sapphire substrate as compared to films grown on Hastelloy substrates [8], [9].

In this work, we have developed a 1D electrothermal model using a commercial finite-element software which allowed us to investigate the thermal behavior of various tape architectures as well as their current limitation performance for various fault current levels. A distinct 3D electrothermal model was used to obtain the NZPV of the tape architectures investigated.

II. 1D ELECTROTHERMAL MODEL

The 1D electrothermal model calculates the current and the temperature in a HTS tape at the location of a hot spot. The dimension simulated corresponds to the thickness of the HTS tape. At the beginning of the simulation, the model assumes that the HTS has quenched at the hot spot(s) location(s). Finite elements simulations are performed using the heat transfer module of the COMSOL Multiphysics 4.3b software package. The variable solved by the software is the temperature T and is calculated using the heat equation, which reads:

$$\rho_m C_p(T) \frac{\partial T}{\partial t} + \nabla \cdot (-k(T) \nabla T) = Q_j, \quad (1)$$

where ρ_m is the mass density, $C_p(T)$ is the heat capacity, $k(T)$ is the thermal conductivity and Q_j represent the Joule losses, that is to say:

Manuscript received October 30, 2018. This project has received funding from the European Union's Horizon 2020 research and innovative program under grant agreement No 721019. The authors are grateful to THEVA for providing the experimental data used in the simulations.

C. Lacroix and F. Sirois are with Polytechnique Montréal, Montréal, QC, H3T 1J4, Canada (e-mails: christian.lacroix@polymtl.ca, f.sirois@polymtl.ca).

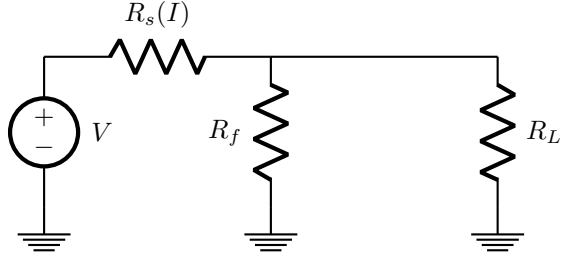


Fig. 1. Electrical network used to simulate a fault current.

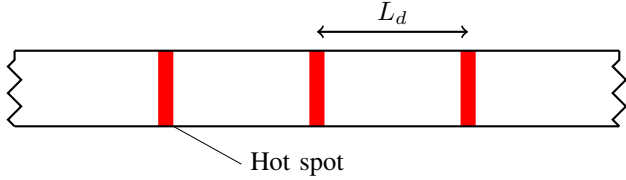


Fig. 2. The model assumes that the distance between the hot spots (L_d) is the same all along the tape.

$$Q_j = \rho(T) J^2. \quad (2)$$

We assume no heat exchange between the HTS tape and its surrounding (adiabatic conditions). The following Neumann boundary condition is thus applied on both surfaces of the tape:

$$\mathbf{n} \cdot \nabla T = 0. \quad (3)$$

The electrical behavior of the DC network is modeled by a voltage source connected to two resistances in series: the first resistance R_s represents the SFCL, whose value depends on the current flowing in the SFCL, and the second resistance R_L represents the impedance of the network in normal conditions (see Figure 1). To simulate a fault current, a resistance R_f is placed in parallel with R_L . The value of R_f is used to adjust the level of the fault current. The total impedance of the network R_n is thus given by

$$R_n = R_s + \frac{R_L R_f}{R_L + R_f}. \quad (4)$$

The voltage V of the electrical network is determined considering the maximum electric field E_{max} that the HTS tape must withstand (150 V/m), the distance between each hot spot L_d and the number of hot spots N , *i.e.*

$$V = E_{max} N L_d. \quad (5)$$

We assume that the hot spots are equally distant (see Figure 2). The impedance R_L of the network in normal conditions is determined by the nominal current I_n in normal conditions, which is set to $0.5I_c$. We thus have

$$R_L = \frac{E_{max} N L_d}{0.5I_c}. \quad (6)$$

The resistance of the SFCL is determined as follows. First, the mean conductivity of the tape in the quenched region is calculated using the following expression:

$$\langle \sigma \rangle = \frac{\sum_i \sigma_i t_i}{\sum_i t_i}, \quad (7)$$

where σ_i and t_i are the conductivity and thickness of the i^{th} layer, respectively. The conductivity σ_i of a layer is determined from the average temperature on its cross-section $\langle T_i \rangle$. We assume that the temperature of the whole quenched region is that of the hot spot. This leads to a slight overestimation of the temperature. We estimated that the error generated by this approximation is less than 5%.

The total resistance of the SFCL is thus expressed as

$$R_s = \frac{L_{nz}}{\langle \sigma \rangle S}, \quad (8)$$

where L_{nz} is the total length of the tape in a quenched state, and S is the total area of the cross-section of the tape, which is given by $S = \sum_i w t_i$, where w is the width of the tape.

The total length L_{nz} of the tape that is quenched is given by $N \min(2t v_{nz}, L_d)$, where t is the time elapsed after the generation of the first normal zone and v_{nz} is the NZPV. The factor of 2 represents the fact that the normal zone propagates in both directions along the length of the tape.

Calculations of the NZPV for each tape architecture considered here are detailed in the next section. As we will see, v_{nz} varies with the applied current. In the 1D electrothermal model, the value of v_{nz} is considered constant during the whole simulation. Its value is fixed at the beginning of the simulation using the value of the prospective fault current I_f , where $I_f = V(R_f + R_L)/(R_f R_L)$. We estimate that the error caused by this simplification is less than 10% in the worst case.

Once R_s is known, the total current in the tape is given by $I = V/R_s$. Using the conductivity of each layer σ_i , as well as the respective cross-section of each layer, it is easy to find the current flowing in each layer.

III. HTS CONDUCTOR DESIGN

In this work, we first targeted potential tape architectures that met our temperature safety criterion for the two extremes cases: clear fault and hot spot. The temperature safety criterion was chosen to be 425 K. Therefore, we performed numerical calculations in clear fault and hot spot conditions for various possible architectures and, based on the results, we chose three promising architectures (see Table I).

Regarding the materials used, we explore several combinations. The superconducting material consisted of a 3.3 μm -thick GdBaCuO (or GBCO) layer. For the substrate, two types of material were considered: Hastelloy and sapphire. While Hastelloy is commonly used in the fabrication of 2G HTS CCs, it is only recently that it was reported that cuprate superconductors could be grown on long length (more than 1 meter) sapphire ribbons [1], [10]. For all architectures, we assumed the presence of a silver layer whose thickness was at least 500 nm on the GBCO layer. Finally, we explored several

TABLE I
 COMPOSITION OF CHOSEN TAPE ARCHITECTURES. THE THICKNESSES OF EACH LAYER ARE GIVEN IN PARENTHESIS.

Architecture	Substrate	Silver	Shunt
1	Hastelloy (500 μm)	Surround (0.5 μm)	Tin solder (2 μm) + Hastelloy (500 μm)
2	Hastelloy (100 μm)	Surround (1 μm)	Tin solder (10 μm) + Hastelloy (500 μm) + Surround Steelcast (300 μm)
3	Sapphire (3000 μm)	GBCO side only (8 μm)	Y ₂ O ₃ (500 μm)

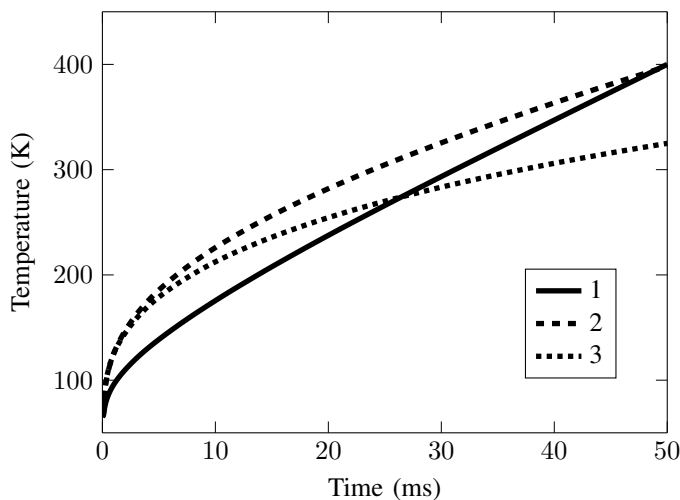


Fig. 3. Maximum temperature calculated in the GBCO layer over time during a clear fault. (See Table I for the details of tape architectures 1, 2 and 3)

types of shunt such as Hastelloy (soldered with tin), Steelcast (mix of stycast and micron-sized stainless steel particles) [11] and Y₂O₃. The material properties of Hastelloy, tin, sapphire, Y₂O₃ and silver are easily found in COMSOL materials data base or in the literature [12], [5], [13]. The thermal properties of GBCO were taken from [14].

Finally, we assumed that the HTS tape was immersed in a subcooled liquid nitrogen bath whose temperature is 65 K. At $T = 65$ K, the I_c of a 3.3 μm -thick and 12 mm wide GdBaCuO layer was set to 1265 A.

To simulate the clear fault scenario, we set $R_f = 0$, meaning that the whole voltage develops in the SCFL. The resulting maximum temperature in the GBCO layer over time is given in Figure 3, while the current in the tape over time is given in Figure 4.

We observe that the temperature reached after 50 ms is 400 K or below, which satisfies our safety temperature criterion of 425 K. We note that the maximum temperature in the clear fault scenario is lower for architecture 3. This is due to the increase of silver resistivity when temperature increases, in contrary to Hastelloy, whose resistivity is nearly temperature independent. This is also seen in Figure 4 where the current decreases faster in the case of architecture 3. However, the peak current is much higher in case of architecture 3 (≈ 4 kA)

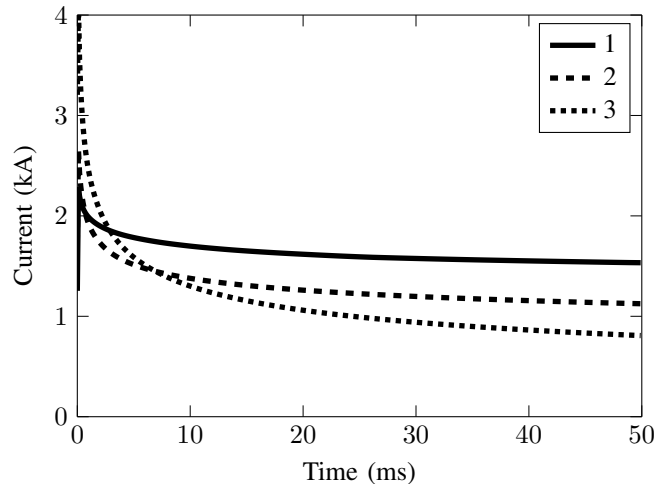


Fig. 4. Total network current over time during a clear fault.

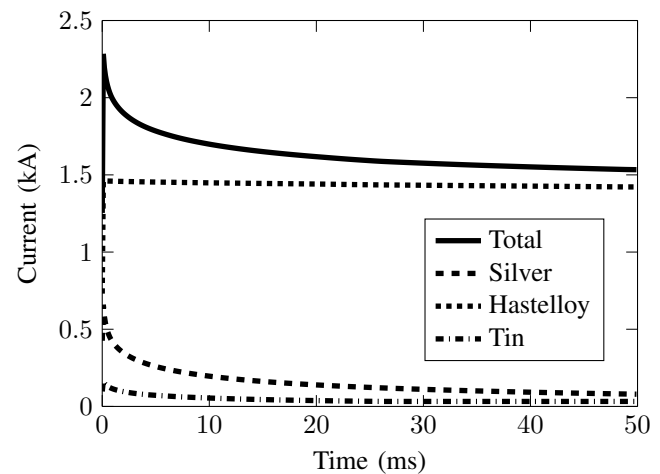


Fig. 5. Example of current sharing between layers of architecture #1 in the case of a clear fault.

in comparison with architectures 1 and 2 (≈ 2.3 kA for architecture 1 and ≈ 2.7 kA for architecture 2).

An example of current sharing between the layers of architecture 1 in the case of a clear fault is presented in Figure 5. We observe that most of the current flows in the Hastelloy layers since more than 99% of the volume of the tape is made from Hastelloy. Since the electrical conductivity of Hastelloy is almost temperature-independent, the amount of current flowing into it stays the same as time progresses (and temperature increases), as opposed to what happens in the silver and tin layers.

The hot spot scenario assumed that a single hot spot was generated. Furthermore, we assumed that the fault current amplitude was equal to I_c (1265 A) and was constant over time. This was implemented in the model by setting $R_s = 0$ and $R_f = R_L$. The maximum temperatures over time for all architectures are presented in Figure 6. We observe that the maximum temperature is lower than our safety temperature criterion (425 K) for all architectures. We also note that the maximum temperature of architecture 1 after 50 ms is much

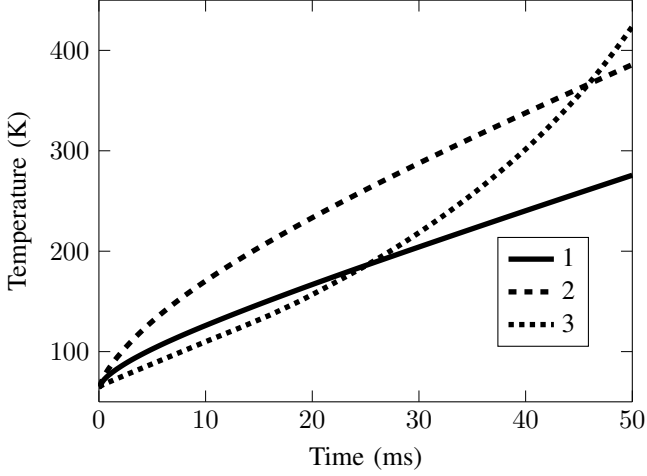


Fig. 6. Maximum temperature calculated in the GBCO layer over time in presence of a single hot spot. The applied current is constant over time and is equal to the critical current (1265 A).

lower than that of architectures 2 and 3. This can be explained by the lower resistance per meter of architecture 1.

IV. EVALUATION OF THE NZPV

In order to obtain the NZPV, three-dimensional finite element simulations were run in the Joule heating module of the COMSOL Multiphysics 4.3b software package. Details of the model can be found in Refs. [5], [7]. The variables solved for in the model were the electrical potential V and the temperature T , and were calculated using the current continuity equation and heat equation, respectively. The current $I(t)$ was imposed at one end of the tape while the other end was grounded.

The electrical conductivity of GBCO in the flux creep and flux flow regimes was approximated by a power-law model, while the transition from the superconducting state to the normal state was modeled assuming two resistances in parallel. Explicitly, the equations used in the model for the electrical properties of GBCO in the superconducting state were

$$\sigma_{GBCO}(T) = \sigma_{sc}(T) + \sigma_n(T), \quad (9)$$

$$\sigma_{sc}(T) = \frac{J_c(T)}{E_0} \left(\frac{\|E\|}{E_0} \right)^{\frac{1-n(T)}{n(T)}}, \quad (10)$$

where $\sigma_{sc}(T)$ is the conductivity in the superconducting state, $\sigma_n(T)$ is the conductivity in the normal state, $J_c(T)$ is the critical current density, $\|E\|$ is the norm of the electric field, E_0 is the electric field criterion and $n(T)$ is a fitting parameter.

The critical current density J_c and n -factor of GBCO in self-field have been obtained experimentally over a temperature range from 25 K up to 90 K. They were fitted with polynomial functions. The polynomial functions included in the model were:

$$J_c(T) = 4.016 \times 10^{-5} T^4 - 8.9 \times 10^{-3} T^3 + 7.256 \times 10^{-1} T^2 - 35.7T + 1189, \quad (11)$$

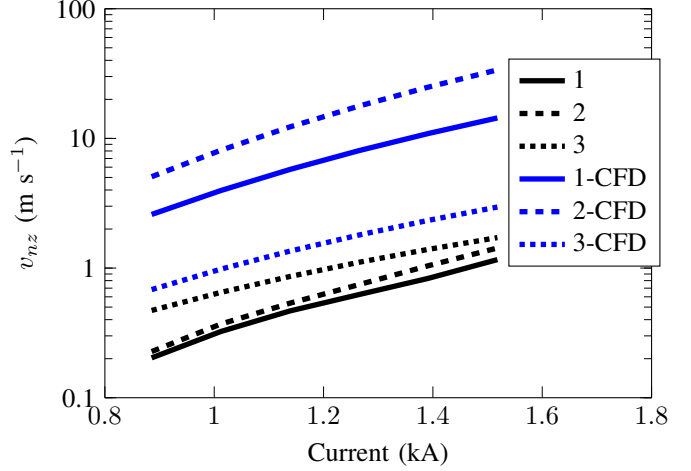


Fig. 7. Dependence of the NZPV with the applied current for all three architectures with and without a CFD.

$$n(T) = 2.99 \times 10^{-7} T^5 + 7.546 \times 10^{-5} T^4 - 7.844 \times 10^{-3} T^3 + 4.259 \times 10^{-1} T^2 - 12.12T + 183.4. \quad (12)$$

The dependence of the NZPV with current for our three architectures was first obtained. Results are presented in Figure 7 (black lines). The value of the NZPV varied approximately from 0.2 m/s up to 1.7 m/s depending on the applied current. We note that architecture 3 possesses a higher NZPV thanks to its sapphire substrate.

Simulations were also realized for the case where a CFD consisting of a resistive layer covering 90% of the GBCO/Ag interface was inserted in the tape (blue lines in Figure 7). In the case of architectures 1 and 2, the addition of a CFD increases the NZPV by more than one order of magnitude and NZPVs of more than 30 m/s are predicted. In the case of architecture 3, the gain due to the addition of a CFD is less important and corresponds to a gain factor of approximately 1.5.

V. CURRENT LIMITATION IN A HVDC NETWORK

In Figure 8, we present the maximum temperature over time calculated with the 1D model in the case where the prospective fault current equals the critical current and hot spots are generated every meter ($L_d = 1$ m). Comparing with the case of a single hot spot (Figure 6), we observe that the temperatures reached after 50 ms are slightly lower in the case of architectures 1 and 2. In the case of architecture 3, the difference is larger (≈ 100 K). The reason is due to the higher NZPV of architecture 3 in comparison with architectures 1 and 2 (see Figure 7). The corresponding limited current is presented in Figure 9. While the current limitation is rather small for architectures 1 and 2, architecture 3 is more efficient to limit the current due to its higher NZPV. We note also that, for all three architectures, the quench is only partial after 50 ms.

We have seen before (Figure 7) that the insertion of a CFD in a HTS tape can drastically increase the NZPV. In Figure 10, the maximum temperature in the GBCO layer over time is

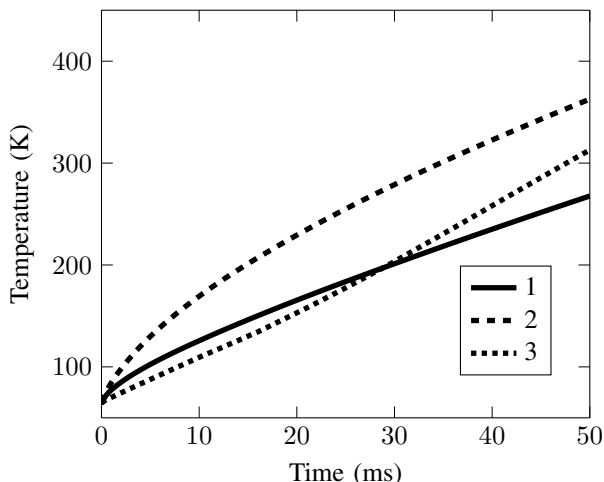


Fig. 8. Maximum temperature calculated in the GBCO layer over time in presence of hot spots located at each meter ($L_d = 1$ m). The prospective fault current is equal to the critical current ($R_f = R_L$).

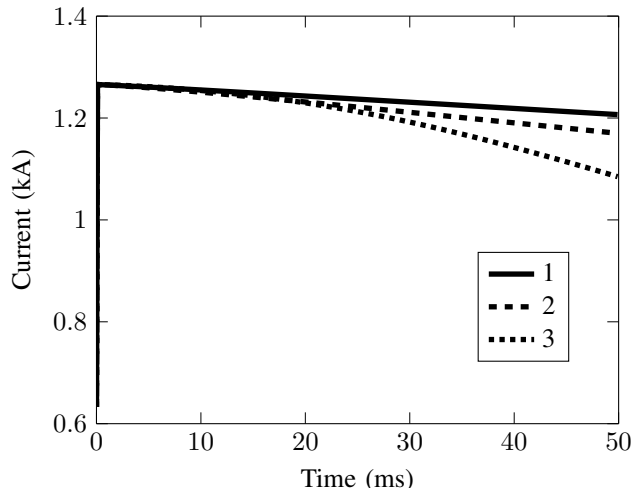


Fig. 9. Limited current over time in presence of hot spots located at each meter ($L_d = 1$ m). The prospective fault current is equal to the critical current ($R_f = R_L$).

presented for the same parameters as those used for generating Figure 8, except for the NZPV, which is the one calculated in presence of a CFD. We first observe that the temperature reached after 50 ms is lower for all three architectures when a CFD is included. Furthermore, in Figure 11, we observe that the current limitation is more efficient in presence of a CFD. The higher efficacy is a consequence of the higher NZPV induced by the CFD. For example, in the case of architecture 2, the tape becomes fully quenched at $t \approx 28$ ms (dashed line in Figure 11) and the current corresponds to $\approx 55\%$ of the prospective fault current. This is clearly seen by the change of slope in the variation of the current with time. When no CFD is present in architecture 2 (Figure 9), the limitation of the current is much less effective (the current corresponds to $\approx 93\%$ of the prospective current). This explains why the temperature is much higher in this case after 50 ms: 363 K (no CFD) versus 210 K (with CFD). Regarding architecture 1, similar trends are observed despite the fact that the current limitation is a bit less effective than with architecture 2. In the case of architecture 3 (sapphire substrate), adding a CFD provides benefits but to a lesser extent. Indeed, as discussed earlier, in the case of architecture 3, the gain in NZPV due to the insertion of a CFD is less important.

We now investigate the effect of the hot spot interdistance. Basically, in our model, when the hot spot interdistance is lower, it corresponds to a higher density of hot spots. In reality, the hot spot interdistance is correlated to the applied current, *i.e.* $L_d(I)$, and the relationship between L_d and I depends on the distribution of I_c along the length of the tape. Indeed, as the current increases, more and more regions of a HTS tape will quench. However, quantitative values of L_d requires knowing the local I_c along the whole length of the tape, but we don't have this information at the moment.

In Figure 12, the temperature of a hot spot is given versus the hot spots interdistance when the prospective fault current is equal to the critical current. We observe that the temperature is lower when the hot spot interdistance is small (less than

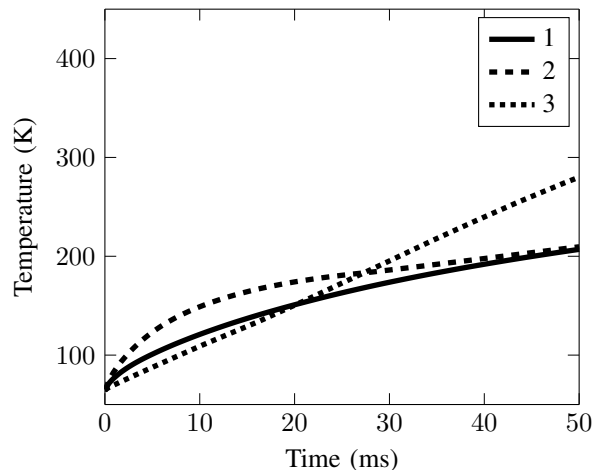


Fig. 10. Maximum temperature calculated in the GBCO layer over time in presence of hot spots located at each meter ($L_d = 1$ m) in presence of a CFD. The prospective fault current is equal to the critical current ($R_f = R_L$).

1 cm). The reason is that the tape becomes fully quenched in a timeframe of less than 50 ms, *i.e.* $v_{nz}L_d < 50$ ms. If the hot spots interdistance is between 1 cm and 1 m, the hot spot temperature increases. The reason is that the NZPV is not high enough to fully quench the tape. Finally, we observe that the temperature of a hot spot is much higher as the density of hot spots becomes lower ($L_d > 10$ m) and temperatures similar to the single hot spot case are found (see Figure 6).

When a CFD is integrated in the tape architecture (Figure 13), we observe that the gain in NZPV allows reducing considerably the temperature elevation for a low hot spot density, which reduces the probability of damaging the tape. However, we observe that the temperature reached after 50 ms for $L_d > 10$ m is very close again to the temperature obtained for the single hot spot case. This indicates that even if the CFD gives increased robustness, the gain in NZPV due to the CFD is not sufficient to protect the tape in the extreme case of a single hot spot.

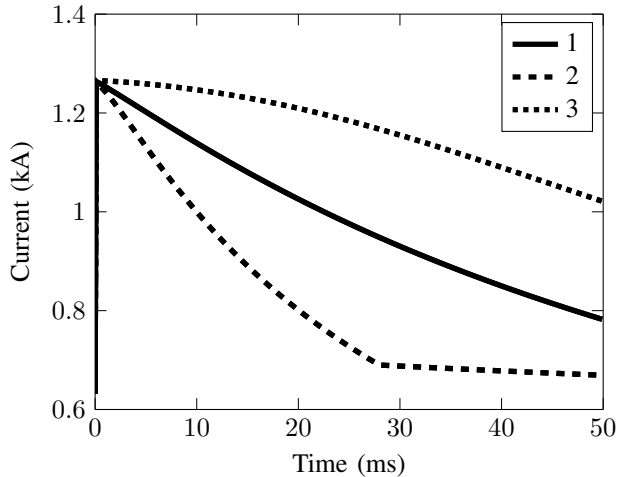


Fig. 11. Limited current over time in presence of hot spots located at each meter ($L_d = 1$ m) in presence of a CFD. The prospective fault current is equal to the critical current ($R_f = R_L$).

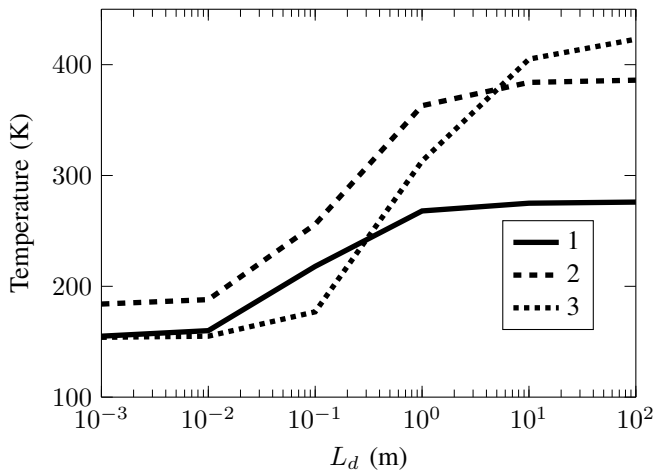


Fig. 12. Maximum temperature calculated in the GBCO layer in presence of hot spots at $t = 50$ ms for various L_d . The prospective fault current is equal to the critical current ($R_f = R_L$).

VI. CONCLUDING REMARKS

We developed a 1D electrothermal model to simulate the behavior of a SFCL in a DC electrical network. Firstly, the two extreme cases of fault current, clear fault and single hot spot, were used to design tape architectures whose temperature must remain below a safety temperature criterion in both cases. Different substrates and combination of shunts were considered. While a shunt with high heat capacity and high electrical resistance is preferable in the clear fault scenario, the electrical resistance cannot be too high in order to limit the temperature elevation in the single hot spot scenario. A compromise must then be found to survive the quench in both cases.

The addition of a CFD increases the NZPV, which helps homogenizing the quench and reducing the fault current level and temperature elevation, and thus diminishes the probability of damaging the tape. If one could design a tape architecture with a NZPV of more than roughly 1 km/s, then this would

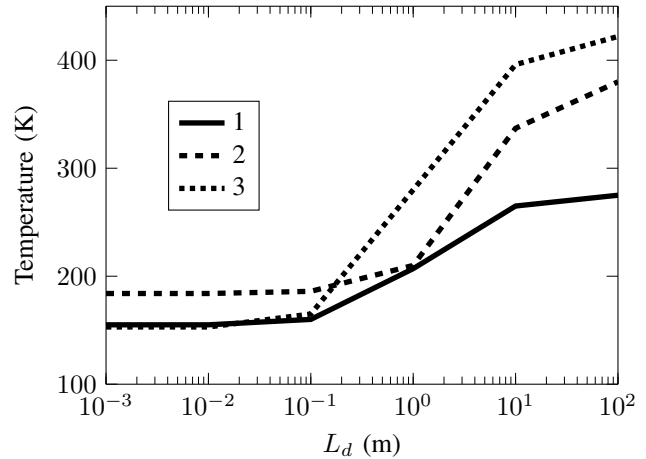


Fig. 13. Maximum temperature calculated in the GBCO layer in presence of hot spots at $t = 50$ ms for various L_d in presence of a CFD. The prospective fault current is equal to the critical current ($R_f = R_L$).

ensure an homogeneous quench of the REBCO within 50 ms even in the worst case scenario of a single hot spot. This would also reduce the temperature elevation in the extreme case of a single hot spot, which in turn, would allow diminishing the total amount of metallic sheath, thus increasing the resistance per meter. Ultimately, a higher resistance per meter requires a smaller amount of GBCO tape which lowers the cost and the size of SCFL.

Eventually, it would be important to develop a more realistic physical model that allows solving V and T in 2D (or even 3D) and that includes a real distribution of I_c in a power systems analysis software such as EMTP-RV. Some efforts have been made towards this goal by Bonnard *et al.* [15]. However, the model developed by Bonnard *et al.* could not include a real distribution of I_c due to meshing constraints. Indeed, the size of the elements at the frontier between the normal zone and the superconducting zone must be sufficiently small to represent adequately the physical phenomena. Thus, if one wants to simulate hot spots that can be generated anywhere in the tape, a very fine mesh must be used everywhere in the tape geometry. However, having a fine mesh over long lengths of tape would required an enormous computation time. One possibility would be to use adaptive mesh refinement methods to reduce computation time.

Finally, an aspect that was not discussed in this work is the dynamics of the generation of hot spot. It is expected that the generation of hot spot will be harder for tape grown on sapphire simply because of its quite high thermal conductivity. This is an aspect that should be taken in consideration in a future work.

REFERENCES

- [1] FASTGRID project. <https://www.fastgrid-h2020.eu>.
- [2] G. Escamez, J. Vialle, C. Bruzek, V. Groe, M. Bauer, and P. Tixador. Numerical Investigations of ReBCO Conductors With High Limitation Electric Field for HVDC SFCL. *IEEE Trans. Appl. Supercond.*, 28(4):1–5, June 2018.

- [3] A. Badel, G. Escamez, and P. Tixador. REBCO FCL Modelling: Influence of Local Critical Current Non-Uniformities on Overall Behavior for Various Tape Architectures. *IEEE Trans. Appl. Supercond.*, 25(3):1–4, June 2015.
- [4] D. Colangelo and B. Dutoit. Analysis of the influence of the normal zone propagation velocity on the design of resistive fault current limiters. *Supercond. Sci. Technol.*, 27(12):124005, 2014.
- [5] C. Lacroix and F. Sirois. Concept of a current flow diverter for accelerating the normal zone propagation velocity in 2G HTS coated conductors. *Supercond. Sci. Technol.*, 27:035003, 2014.
- [6] C. Lacroix, Y. Lapierre, C. Coulombe, and F. Sirois. High normal zone propagation velocity in second generation high-temperature superconductor coated conductors with a current flow diverter architecture. *Supercond. Sci. Technol.*, 27:055013, 2014.
- [7] C. Lacroix, F. Sirois, and J-H. Fournier Lupien. Engineering of second generation HTS coated conductor architecture to enhance the normal zone propagation velocity in various operating conditions. *Supercond. Sci. Technol.*, 30(6):064004, 2017.
- [8] F. Roy, M. Therasse, B. Dutoit, F. Sirois, L. Antognazza, and M. Decroux. Numerical Studies of the Quench Propagation in Coated Conductors for Fault Current Limiters. *IEEE Trans. Appl. Supercond.*, 19(3):2496–2499, June 2009.
- [9] L. Antognazza, M. Therasse, M. Decroux, F. Roy, B. Dutoit, M. Abplanalp, and O. Fischer. Comparison between the behavior of HTS thin film grown on sapphire and coated conductors for fault current limiter applications. *IEEE Trans. Appl. Supercond.*, 19(3):1960, 2009.
- [10] G. Deustcher, M. Azoulay, B. Almog, and A. Saraf. Dielectric substrate for superconductive device and superconductive article utilizing such substrate, 2017/0004913A1 5 Jan. 2017.
- [11] E. J. Wollack, D. J. Fixsen, R. Henry, A. Kogut, M. Limon, and P. Mirel. Electromagnetic and thermal properties of a conductively loaded epoxy. *International Journal of Infrared and Millimeter Waves*, 29(1):51–61, Jan 2008.
- [12] COMSOL Multiphysics v. 4.3b. www.comsol.com, COMSOL AB, Stockholm, Sweden.
- [13] F. Roy. *Modeling and Characterization of Coated Conductors Applied to the Design of Superconducting Fault Current Limiters*. PhD thesis, École Polytechnique Fédérale de Lausanne, 2010.
- [14] Database for thermal and mechanical properties of REBaCuO bulks. *Physica C Supercond.*, 426-431:699 – 704, 2005.
- [15] C.-H. Bonnard, F. Sirois, C. Lacroix, and G. Didier. Multi-scale model of resistive-type superconducting fault current limiters based on 2G HTS coated conductors. *Supercond. Sci. Technol.*, 30(1):014005, 2017.